

A New Class of Stereoregular Vinylene-Arylene Copolymers with Double-Decker Silsesquioxane in the Main Chain

Patrycja Żak,¹ Beata Dudzic,¹ Michał Dutkiewicz,² Monika Ludwiczak,² Bogdan Marciniec,² Marek Nowicki³

¹Department of Organometallic Chemistry, Faculty of Chemistry, Adam Mickiewicz University in Poznan, Umultowska 89B, 61-614 Poznan, Poland

²Centre for Advanced Technologies, Adam Mickiewicz University in Poznan, Umultowska 89C, 61-614 Poznan, Poland

³Institute of Physics, Poznan University of Technology, Piotrowo 3, 60-965 Poznan, Poland

Correspondence to: B. Marciniec (E-mail: Bogdan.Marciniec@amu.edu.pl)

Received 27 July 2015; accepted 1 October 2015; published online 12 November 2015

DOI: 10.1002/pola.27957

ABSTRACT: A synthesis of a new macromolecular class of vinylene-arylene copolymers with double-decker silsesquioxane in the main chain is presented. Two transition-metal-catalyzed processes, which is silylative-coupling copolycondensation (SCC) and ADMET copolymerization of divinyl-substituted double-decker silsesquioxanes (DDSQ-2SiVi) with selected diolefins, are reported to be highly efficient tools for the formation of stereoregular copolymers containing DDSQ-silylene-vinylene-

arylene units. The copolymeric products are studied in terms of their structural, thermal, and mechanical properties. © 2015 Wiley Periodicals, Inc. *J. Polym. Sci., Part A: Polym. Chem.* **2016**, *54*, 1044–1055

KEYWORDS: ADMET copolymerization; double-decker silsesquioxane; DSC; GPC; hybrid polymers; NMR; silylative coupling copoly condensation; TGA

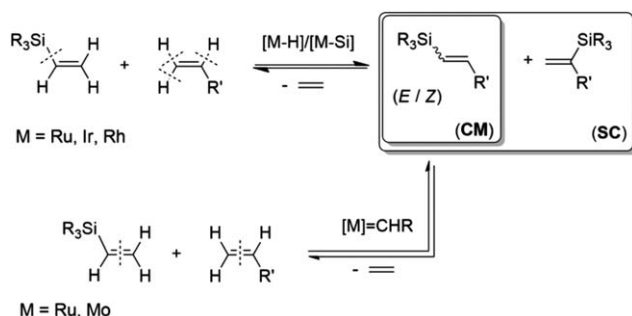
INTRODUCTION Polyhedral oligomeric silsesquioxanes (POSS), which consist of a rigid inorganic SiO core with flexible and reactive and/or inert organic coronae, have attracted much attention because of their unique structures, in addition to their physical properties such as low dielectric constant and high thermal stability.¹ The well-defined organization of POSS is important due to its possible use as a precursor and component of versatile inorganic/organic hybrid materials, also displaying nanophase behavior. Just over a decade ago, the POSS group has been extended by another class of silsesquioxyl compounds containing rigid Si-O-Si bonds, the double-decker silsesquioxane (DDSQ). The efficient synthesis of this compound and its first derivatives was performed by Yoshida and co-workers.² The structure of double-decker silsesquioxane is different from that of the symmetric cubic T₈ system, that is, it is a structure that consists of two “decks” of cyclosiloxane rings stacked on top of one another with eight inert phenyl groups at the silicon atoms of each ring. These two rings are joined by oxygen bridges. In recent years, it has been shown that the syntheses of molecular and macromolecular organosilicon compounds based on DDSQ have led to two major trends in their development and our understanding of their characteristics. The first trend concerns synthesis of molecular DDSQ-

based compounds that possess interesting amphiphilic,³ thermal,⁴ or optic properties⁵ as well as complexes in coordination chemistry.⁶ Another tendency is displayed in the preparation of macromolecular DDSQ-based materials, often with the silsesquioxane in the main chain of the hybrid materials exhibiting interesting and desirable chemical and physical properties.⁷

Over the last two decades, we have been studying and developing two particular types of transition metal-catalyzed reactions, that is, silylative coupling (SC) and cross-metathesis (CM). These processes have proved to be effective routes for synthesis of both molecular and macromolecular compounds with vinylsilicon functionality.⁸ The mechanisms of these two reactions are different, as they exploit different catalysts (mostly ruthenium hydride for SC and ruthenium-carbene for CM). SC occurs via cleavage of the =C-H bond of the olefin and the C-Si bond of vinylsilanes. On the other hand, CM starts with the same substrates (apart from methyl group at silicon atom) and results in a mixture of mostly the same main products, but is preceded by cleavage of the C=C bonds (Scheme 1).

The two above reactions (SC and CM) catalyzed by ruthenium complexes appeared to be complementary methods for

Patrycja Żak and Beata Dudzic contributed equally to this work.
© 2015 Wiley Periodicals, Inc.



SCHEME 1 Silylative coupling (SC) and cross-metathesis (CM) of vinylsilanes with olefins.

regio- and stereoselective functionalization of vinylsilsesquioxanes and vinylspherosilicates.⁹ Next, CM of vinylsilsesquioxanes catalyzed by Grubbs catalyst were also reported by Laine *et al.*,¹⁰ by Naka *et al.*¹¹ as well as by Cole-Hamilton and co-workers.¹² Feher *et al.* used Schrock molybdenum catalyst but, in all reactions except styrene (moderate isolated yields), mixtures of stereoisomers were obtained.¹³ Hydrosilylation and Heck reactions were also studied by means of a new method for vinyl-substituted POSS modification yielding products of interesting photophysical properties and precursors for sugars and peptide scaffolds.^{12(a),14} Last year, we demonstrated a new and elegant method for functionalizing divinyl-substituted double-decker silsesquioxanes (DDSQ-2SiVi) via highly effective SC and/or CM with olefins (Scheme 2).¹⁵ Both reactions proceeded highly stereoselectively and resulted in the formation of *E* isomers. In the case of divinylbenzene (DVB), preliminary studies on its silylative coupling copolycondensation (SCC) with DDSQ-2SiVi leading to synthesis of stereoregular cooligomer containing double-decker (silsesquioxyl-silylene)-vinylene-phenylene units were presented.

In this article, we focus on demonstrating efficient and stereoselective routes, that is, SCC and metathetic copolymerization (ADMET) copolymerization of DDSQ-2SiVi with selected diolefins for the synthesis of a new class of stereoregular vinylene-arylene copolymers with a double-decker silsesquioxane unit in the main chain. The polymeric products were thoroughly characterized via spectroscopic meth-

ods and their structural, thermal, and mechanical properties have also been studied.

EXPERIMENTAL

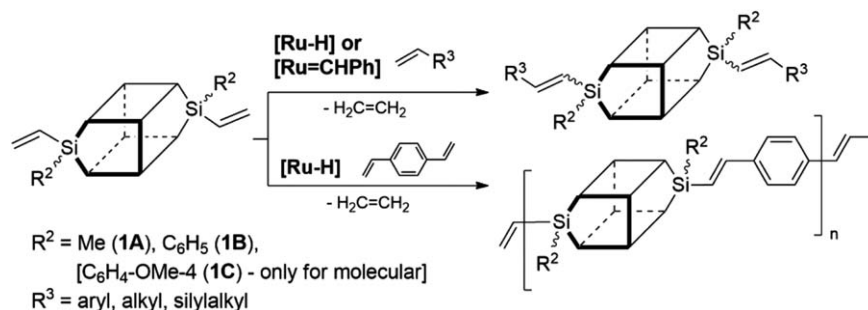
Materials and General Methods

All syntheses and catalytic tests were conducted under argon atmosphere using standard Schlenk-line and vacuum techniques. The chemicals were purchased from the following sources: dichloromethane (DCM), tetrahydrofuran (THF), diethyl ether, ethanol, toluene, *n*-hexane, benzene-*d*₆, chloroform-*d*, tricyclohexylphosphine, potassium carbonate, tetrakis(triphenylphosphine)-palladium(0) [Pd(PPh₃)₄], 1,4-dibromobenzene, potassium *tert*-butoxide, terephthalic aldehyde, methyltriphenylphosphonium bromide, 1,5-cyclooctadiene, 4-bromostyrene, 4-vinylphenylboronic acid, calcium hydride, molecular sieves, and anhydrous magnesium sulfate from Aldrich, vinylmethylchlorosilane and vinylphenyl dichlorosilane from ABCR, triethylamine and silica gel 60 from Fluka, tetrasilanolphenyl POSS (DDSQ-4OH) from Hybrid Plastics, Grubbs first-generation benzylidene catalyst from Apeiron Synthesis, ruthenium(III) chloride hydrate from Lancaster. [RuHCl(CO)(PCy₃)₂],¹⁶ as well as divinyl-substituted double-decker silsesquioxanes (DDSQ-2Vi) (**1A**, **1B**)^{15,17} were prepared according to the literature procedure. All solvents were dried over CaH₂ prior to use and stored under argon over type 4A molecular sieves. DCM was additionally passed through a column with alumina and then it was degassed by repeated freeze-pump-thaw cycles.

Measurements

¹H, ¹³C, and ²⁹Si nuclear magnetic resonance (NMR) spectra were recorded at 298 K on Varian 400 (402.6 and 101.2 MHz), and Bruker Avance 400 and 500 (119.3 MHz) spectrometers using CDCl₃ as a solvent. Chemical shifts are reported in ppm with reference to the residual solvent (CHCl₃) peaks for ¹H and ¹³C and to TMS for ²⁹Si.

Mass spectra of the olefins were acquired by gas chromatograph mass spectrometer (GCMS) analysis [Varian Saturn 2100T, equipped with a BD-5 capillary column (30 m)] and an ion trap detector. High-resolution mass spectroscopic (HRMS) analyses were performed on an AMD-402 mass spectrometer.



SCHEME 2 Reaction path for synthesis of molecular and macromolecular DDSQ-based systems via stereoselective silylative coupling (also copolycondensation) and metathetic transformations.

Fourier transform infrared (FTIR) spectra were recorded on a Bruker Tensor 27 Fourier transform spectrophotometer equipped with a SPECAC Golden Gate, diamond ATR unit with a resolution of 2 cm^{-1} .

Thin-layer chromatography (TLC) was conducted on plates coated with 250- μm -thick silica gel and column chromatography was performed on silica gel 60 (70–230 mesh) using hexane/DCM, DCM/water or ether/water.

Gel permeation chromatography (GPC) analyses were performed using a Waters Alliance 2695 system equipped with a Waters 2414 RI detector and a set of three serially connected $7.8 \times 300\text{ mm}$ columns (Waters Styragel HR1, HR2, and HR4). THF was used as a mobile phase in a flow rate of 0.60 mL/min ; column oven temperature was $35\text{ }^\circ\text{C}$ and detector temperature $40\text{ }^\circ\text{C}$. All molecular weight (M_n , M_w) and polydispersity index (PDI) values were calculated based on calibration curve using polystyrene standards (Shodex) in a range from 1.31×10^3 to $3.64 \times 10^6\text{ Da}$. Differential scanning calorimetry (DSC) measurements of approximately 5-mg polymer samples placed in a 40- μL aluminum pan with a pierced lid were carried out under N_2 at a flow rate of 25 mL/min in a range from -90 to $300\text{ }^\circ\text{C}$ at a heating/cooling rate of $10\text{ }^\circ\text{C/min}$ using a DSC-1 (Mettler-Toledo).

Thermogravimetric analysis (TGA) was performed on a TGA Q50 (TA Instruments) analyzer. A sample of a polymer placed on a thermobalance platinum pan was heated from room temperature to $1000\text{ }^\circ\text{C}$ in nitrogen or air flow of 60 mL/min at the heating rate of $10\text{ }^\circ\text{C/min}$.

Water contact angles (WCAs) of polymer-coated stainless steel plates were measured using a Krüss GmbH DSA 100E Drop Shape Analyzer equipped with a software-controlled (DAS4 2.0): x , y , z -axis table, quadruple dosing unit with zoom and focus adjustment, illumination, and a camera with $780 \times 580\text{ px}$ resolution. All presented data are arithmetic means of values measured for 5 drops per sample.

The measurements of the mechanical properties were taken using a nanoindentation technique. This uses a controlled indentation of the diamond tip (indenter) in the sample surface and registers the loading force of the indenter as a function of indentation depth. This method enables the calculation of the hardness and Young's modulus for even very small quantities of material. Measurements were taken on the surface of the resulting copolymer by evaporating the solvent from the drops of the polymer solution applied to the metal plate. The film thickness was in the range of 120 – $150\text{ }\mu\text{m}$. Measurements were performed at a temperature of $20\text{ }^\circ\text{C}$ and at a humidity of 50%. The measurements were taken with Berkovich tip geometry and an Agilent G200 indenter. Measurements were carried out in CSM mode with a DCMII indenter head. The depth of the indentation was limited to 1000 nm . Applied loading curves contain a segment retaining the maximum force for 10 seconds. For each sample, at least 10 tests were performed, and the results were averaged.

Scanning electron microscopy (SEM) images were taken using an FEI Quanta 250 FEG microscope equipped with an EDAX EDS detector. Images were taken in high vacuum mode, and accelerating voltage (5 kV). Samples were prepared by gluing the polymer powder on the standard SEM carbon adhesive tape.

The X-ray diffraction experiments were carried out on The Oxford Diffraction New Xcalibur diffractometer with MoK_α radiation ($\lambda = 0.71073\text{ \AA}$), equipped with a graphite monochromator and a CCD detector (EosS2). A 0.3-mm pinhole collimator was used and the detector was set at 100 mm from the sample. The exposure time was fixed to 300 s per scan and images were collected with a 300° phi rotation. Data collection and reduction were performed with CrysAlis-Pro software.¹⁸

Diolfen Synthesis

1,4-Divinylbenzene

Terephthalic aldehyde (2 g, 14.9 mmol) in THF (20 mL, dry and deoxidized) was added slowly to a suspension of methyltriphenyl phosphonium bromide (12.6 g, 35.3 mmol) and potassium *tert*-butoxide (4.8 g, 42.8 mmol) in THF (20 mL) at 0 – $5\text{ }^\circ\text{C}$ under argon atmosphere. After the addition was completed, the reaction mixture was allowed to stir at room temperature for 4 h, concentrated, and extracted (ether/water). The organic layer was dried over magnesium sulfate(VI) MgSO_4 , concentrated, and poured into hexane (50 mL). The excess of hexane was evaporated and the residue was separated with silica gel column (eluent: hexane). 1,4-DVB was dissolved in a small amount of dried ether and filtrated with Sartorius Minisart syringe filters (PTFE, $0.2\text{ }\mu\text{m}$). The colorless liquid (easily solidifying) was gained after evaporation of ether (1.5 g, yield: 75%).

^1H NMR (300 MHz, C_6D_6 , δ , ppm): 5.25 (d, 2H, $J_{\text{HH}} = 9\text{ Hz}$, $-\text{CH}=\text{CH}_2$), 5.68 (d, 2H, $J_{\text{HH}} = 17.4\text{ Hz}$, $-\text{CH}=\text{CH}_2$), 6.57 (dd, 2H, $J_{\text{HH}} = 11.1, 18.0\text{ Hz}$, $-\text{CH}=\text{CH}_2$), 7.19 (s, 4H, $-\text{C}_6\text{H}_4-$); ^{13}C NMR (75 MHz, C_6D_6 , δ , ppm): 114.12 ($-\text{CH}=\text{CH}_2$), 127.25 ($-\text{C}_6\text{H}_4-$), 137.36 ($-\text{CH}=\text{CH}_2$), 137.96 (C_i from $-\text{C}_6\text{H}_4-$); MS (EI): m/z (rel. intensity - %): 130 (M^+) (100), 115 (39), 103 (10), 89 (5), 77 (12), 63 (15), 51 (20); HRMS (ESI, m/z) Calcd. for $\text{C}_{10}\text{H}_{10}$: 130.07825, found 130.07838.

Synthesis of 4,4'-Divinyl-1,1'-biphenyl and 4,4'-Divinyl-*p*-terphenyl

4,4'-Divinyl-1,1'-biphenyl and 4,4'-divinyl-*p*-terphenyl were synthesized according to already known procedure¹⁹ except for the catalyst which was replaced with commercially available $[\text{Pd}(\text{PPh}_3)_4]$. Toluene (20 mL), ethanol (6.6 mL), and water solution of potassium carbonate (11.7 mL, 2 M) were added, respectively, to a mixture of 4-bromostyrene (16.8 mmol) or 1,4-dibromostyrene (16.8 mmol) and 4-vinylphenylboronic acid (1.68 mmol) or (3.36 mmol), respectively, and $[\text{Pd}(\text{PPh}_3)_4]$ (23 mg, 0.02 mmol, 2 mol %) under argon atmosphere and stirred at $90\text{ }^\circ\text{C}$ for 12 h and catalyst (0.4 mmol, 2 mol %) under argon atmosphere and stirred at $90\text{ }^\circ\text{C}$ for 12 h. Advancement of reaction was controlled with GCMS analysis. The excess of solvents was

evaporated and product was extracted (DCM/water). The organic layer was dried over magnesium sulfate and purified with silica gel column (dichloromethane). The solvent was evaporated to afford 318 mg of 4,4'-divinyl-1,1'-biphenyl (yield 92%) and 427 mg of 4,4'-divinyl-*p*-terphenyl (yield 90%).

4,4'-Divinyl-1,1'-biphenyl

¹H NMR (300 MHz, CDCl₃, δ, ppm): 5.3 (d, 2H, *J*_{HH} = 11.1 Hz, -CH=CH₂), 5.77 (d, 2H, *J*_{HH} = 17.7 Hz, -CH=CH₂), 6.77 (dd, 2H, *J*_{HH} = 11.2, 17.5 Hz, -CH=CH₂), 7.5 (d, 4H, *J*_{HH} = 8.4 Hz, *H*₂), 7.57 (d, 4H, *J*_{HH} = 8.4 Hz, *H*₃); ¹³C NMR (75 MHz, CDCl₃, δ, ppm): 114 (-CH=CH₂), 126.8, 127.1, 136.2 (-CH=CH₂), 136.8, 140.1; MS (EI): *m/z* (rel. intensity - %): 206 (M⁺) (100), 191 (7), 188 (10), 178 (12), 165 (6), 152 (7), 103 (5), 89 (4), 76 (5), 51 (3); HRMS (ESI, *m/z*) calcd. for C₁₆H₁₄: 206.10955, found 206.10948.

4,4'-Divinyl-*p*-terphenyl

¹H NMR (300 MHz, CDCl₃, δ, ppm): 5.3 (d, 2H, *J*_{HH} = 11.1 Hz, -CH=CH₂), 5.81 (d, 2H, *J*_{HH} = 17.7 Hz, -CH=CH₂), 6.77 (dd, 2H, *J*_{HH} = 11.2, 17.5 Hz, -CH=CH₂), 7.5 (d, 4H, *J*_{HH} = 8.4 Hz, *H*₂), 7.62 (d, 4H, *J*_{HH} = 8.4 Hz, *H*₃), 7.7 (s, 4H, *H*₂); ¹³C NMR (75 MHz, CDCl₃, δ, ppm): 114 (-CH=CH₂), 126.9, 127.1, 127.3, 136.4 (-CH=CH₂), 136.5, 136.7, 140.0; MS (EI): *m/z* (rel. intensity - %): 282 (M⁺) (100), 265 (5), 252 (6), 239 (5), 225 (3), 202 (4), 179 (4), 152 (3), 141 (7), 126 (4), 77 (4), 51 (2); HRMS (ESI, *m/z*) calcd. for C₂₂H₁₈: 282.14085, found 282.14077.

Polymer Synthesis

Metathetic copolymerization

A 5-mL glass reactor equipped with a reflux condenser and connected to a gas/vacuum line was charged under argon with DDSQ-2SiVi (1B) (0.15 g, 1.13 × 10⁻⁴ mol), diolefin (1.13 × 10⁻⁴ mol), and DCM (2 mL). The mixture was warmed up in an oil bath to 45 °C and first-generation Grubbs' catalyst (0.0018 g, 2.48 × 10⁻⁶ mol) was added to the mixture under argon. The reaction mixture was heated under reflux for 24 h or 5 days. Then, the solvent was evaporated under a vacuum and cold *n*-hexane (2 mL) was added to the remaining content to form white precipitate. The precipitate was filtered off and purified by column chromatography (silica gel 60/hexane:DCM = 1:5) to remove ruthenium complexes. Evaporation of the solvent allowed an analytically pure sample (white powder) to be obtained.

Silylative Coupling Copolycondensation

A 5-mL glass reactor, equipped with a reflux condenser and connected to a gas/vacuum line, was charged under argon with DDSQ-2SiVi (1A) (0.15 g, 1.24 × 10⁻⁴ mol), diolefin (1Ph, 2Ph) (1.24 × 10⁻⁴ mol), and DCM or toluene for reaction with 4,4'-divinyl-*p*-terphenyl (3 mL). The mixture was warmed up in an oil bath to 45 °C (for reactions performed in DCM) or 100 °C (for reactions performed in toluene) and [RuHCl(CO)(PCy₃)₂] (0.0018 g, 2.48 × 10⁻⁶ mol) was added to the mixture under argon. After 5 min of the reaction copper(I) chloride (0.0012 g, 1.24 × 10⁻⁵ mol) was added. The reaction mixture was heated under reflux for 24 h or 5 days.

Then, the solvent was evaporated under a vacuum and cold *n*-hexane (2 mL) was added to the remaining content to form colorless precipitate. The precipitate was filtered off and purified by column chromatography (silica gel 60/hexane:DCM = 1:5) to remove ruthenium complexes. Evaporation of the solvent allowed an analytically pure sample (white powder) to be obtained.

Co-oligomers Spectroscopic Analysis

1A-1Ph-1

¹H NMR (CDCl₃, δ, ppm): 0.42 (s, 6H, CH₃ from terminal part), 0.5 (b s, 6H, CH₃ from copolymer), 5.92 - 6.26 (m, 6H, -CH=CH₂ from terminal part), 6.52 (d, 2H, *J*_{HH} = 19.0 Hz, =CHSi), 6.95 - 7.84 (m, 46H, =CH-C₆H₄- and C₆H₅); ¹³C NMR (CDCl₃, δ, ppm): -0.72 (CH₃ from terminal part), -0.64 (CH₃ from copolymer), 124.25 (d, *J* = 6.4 Hz), 126.94, 127.32, 127.62 (t, *J* = 7.5 Hz), 127.80, 127.86, 130.29, 130.43, 130.77, 130.90, 131.07, 131.99, 134.02, 134.18 (t, *J* = 4.1 Hz), 136.81, 140.6, 146.08; ²⁹Si NMR (CDCl₃, δ, ppm): -30.19, -30.61, -77.38, -78.26, -79.52, -79.67; isolated yield = 92%

1A-2Ph-5

¹H NMR (CDCl₃, δ, ppm): 0.48 (b s, 6H, CH₃), 6.44 (d, 2H, *J*_{HH} = 19.1 Hz, =CHSi), 6.88 - 7.80 (m, 50H, =CH-(C₆H₄)₂- and C₆H₅); ¹³C NMR (CDCl₃, δ, ppm): -0.67, 124.24 (b s), 126.92, 127.54, 127.60, 127.68, 127.79, 127.87, 129.77, 130.34, 130.41, 130.63, 130.82 (t, *J* = 5.7 Hz), 131.05, 131.97 (d, *J* = 2.2 Hz), 134.01 (b s), 134.05, 134.07, 134.10, 134.16, 134.22, 137.72, 146.17; ²⁹Si NMR (CDCl₃, δ, ppm): -30.27, -78.26, -79.46; isolated yield = 90%

1A-2Ph-1

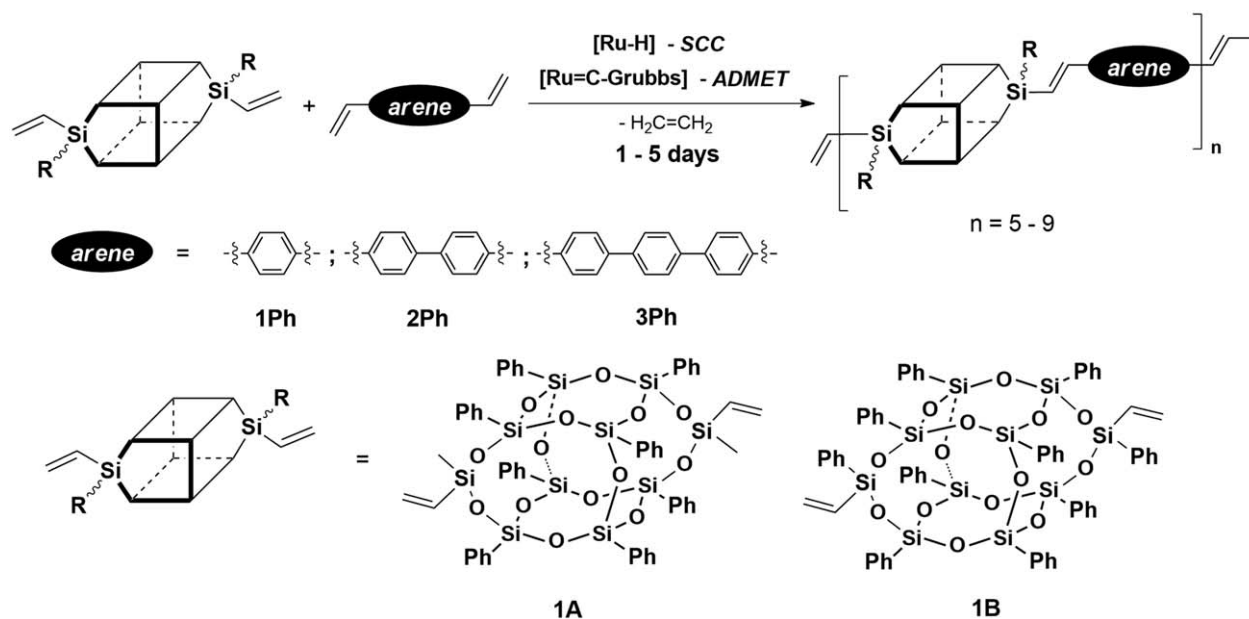
¹H NMR (CDCl₃, δ, ppm): 0.42 (s, 6H, CH₃ from terminal part), 0.5 (b s, 6H, CH₃ from copolymer), 5.93 - 6.26 (m, 6H, -CH=CH₂ from terminal part), 6.52 (d, 2H, *J*_{HH} = 19.2 Hz, =CHSi), 6.77 - 7.86 (m, 46H, =CH-(C₆H₄)₂- and C₆H₅); ¹³C NMR (CDCl₃, δ, ppm): -0.72 (CH₃ from terminal part), -0.64 (CH₃ from copolymer), 124.26 (d, *J* = 7.6 Hz), 126.94, 127.33, 127.61 (t, *J* = 6.6 Hz), 127.81, 127.86, 130.30, 130.43, 130.75, 130.91, 131.08, 131.99, 134.03, 134.14, 134.18, 136.8, 140.61, 146.08; ²⁹Si NMR (CDCl₃, δ, ppm): -30.2, -31.5, -78.26, -79.52, -79.67; isolated yield = 94%

1A-3Ph-5

¹H NMR (CDCl₃, δ, ppm): 0.49 (s, 6H, CH₃), 6.52 (d, 2H, *J*_{HH} = 19.3 Hz, =CHSi), 6.75 - 7.82 (m, 54H, =CH-(C₆H₄)₃- and C₆H₅); ¹³C NMR (CDCl₃, δ, ppm): -0.72, 124.25 (b s), 126.98, 127.37, 127.61 (t, *J* = 6.8 Hz), 127.79, 127.85, 130.30, 130.42, 130.52, 130.60, 130.89, 131.08, 131.99, 134.02, 134.18 (t, *J* = 4.6 Hz), 136.79, 140.52, 146.10; ²⁹Si NMR (CDCl₃, δ, ppm): -30.22, -78.27, -79.51; isolated yield = 91%

1A-3Ph-1

¹H NMR (CDCl₃, δ, ppm): 0.41 (s, 6H, CH₃ from terminal part), 0.5 (b s, 6H, CH₃ from copolymer), 5.91 - 6.24 (m, 6H, -CH=CH₂ from terminal part), 6.51 (d, 2H, *J*_{HH} = 19.2 Hz, =CHSi), 6.76 - 7.81 (m, 54H, =CH-(C₆H₄)₃- and C₆H₅); ¹³C NMR (CDCl₃, δ, ppm): -0.73 (CH₃ from terminal part), -0.64 (CH₃ from copolymer), 124.29 (b s), 126.93, 127.32,



SCHEME 3 General procedure for synthesis of stereoregular co-oligomers with double-decker silsesquioxanes as a spacer via SCC and ADMET reactions of **DDSQ-2SiVi (1A, 1B)** with diolefins.

127.61 (t, $J = 7.5$ Hz), 127.79, 127.85, 130.30, 130.43, 130.61, 130.77, 130.90, 131.07, 131.99, 134.02, 134.17 (t, $J = 4.2$ Hz), 136.8, 140.6, 146.07; ^{29}Si NMR (CDCl_3 , δ , ppm): -30.2, -78.27, -79.52; isolated yield = 89%

1B-1Ph-5

^1H NMR (CDCl_3 , δ , ppm): 6.55 (d, 2H, $J_{\text{HH}} = 19.2$ Hz, =CHSi), 6.97 - 7.76 (m, 56H, =CH-C₆H₄- and C₆H₅); ^{13}C NMR (CDCl_3 , δ , ppm): 122.64, 126.98, 127.46 (t, $J = 10.8$ Hz), 127.80, 127.85, 130.15, 130.26, 130.33, 130.46 (d, $J = 6.5$ Hz), 130.55, 131.66, 134.02, 134.04, 134.11, 137.68, 147.52; ^{29}Si NMR (CDCl_3 , δ , ppm): -44.62, -77.97, -79.34; isolated yield = 95%

1B-1Ph-1

^1H NMR (CDCl_3 , δ , ppm): 6.53 (d, 2H, $J_{\text{HH}} = 18.6$ Hz, =CHSi), 6.93 - 7.75 (m, 56H, =CH-C₆H₄- and C₆H₅); ^{13}C NMR (CDCl_3 , δ , ppm): 124.05, 126.86, 127.59 (t, $J = 10.8$ Hz), 127.81, 130.41, 130.48, 130.59, 130.82, 131.71, 133.84, 133.88, 137.71, 146.17; ^{29}Si NMR (CDCl_3 , δ , ppm): -44.56, -77.92, -79.29; isolated yield = 93%

1B-2Ph-5

^1H NMR (CDCl_3 , δ , ppm): 6.61 (d, 2H, $J_{\text{HH}} = 19.4$ Hz, =CHSi), 6.95 - 7.80 (m, 60H, =CH-(C₆H₄)₂- and C₆H₅); ^{13}C NMR (CDCl_3 , δ , ppm): 122.60, 126.91, 127.42, 127.50, 127.59, 127.87, 130.12, 130.16, 130.21, 130.30, 130.44, 130.47, 130.62, 131.72, 134.07, 134.16, 136.67, 147.51; ^{29}Si NMR (CDCl_3 , δ , ppm): -44.55, -77.96, -79.40; isolated yield = 90%

1B-2Ph-1

^1H NMR (CDCl_3 , δ , ppm): 6.62 (d, 2H, $J_{\text{HH}} = 19.2$ Hz, =CHSi), 6.89 - 7.83 (m, 60H, =CH-(C₆H₄)₂- and C₆H₅); ^{13}C NMR (CDCl_3 , δ , ppm): 122.62, 126.92, 127.43, 127.51, 127.60, 127.87, 128.43, 129.76, 130.22, 130.26, 130.49, 130.62,

131.72, 134.08, 134.17 (t, $J = 3.9$ Hz), 136.70, 140.67, 147.52; ^{29}Si NMR (CDCl_3 , δ , ppm): -44.55, -77.97, -79.39; isolated yield = 92%

RESULTS AND DISCUSSION

Synthesis of Polymers—ADMET Copolymerization and Silylative Coupling Copolycondensation

The SC and CM reaction optimization for a variety of olefins performed and presented in our previous paper enabled efficient synthesis of a series of new, functionalized double-decker-based silsesquioxanes.¹⁵ The positive results from the preliminary test of the SCC of **DDSQ-2SiVi (1A)** with **DVB** prompted us to extend this procedure not only to new diolefins, but also to the utilization of a complementary catalytic reaction, that is, **ADMET** copolymerization. The overview of this process is presented in Scheme 3. As expected,^{15,20} the **DDSQ-2SiVi** containing a methyl group located at Si-9 and Si-19 atoms (**1A**) was confirmed to be inactive in metathetic transformations. For this reason, **ADMET** copolymerization of the **DDSQ-2SiVi** with phenyl group at Si-9 and Si-19 atoms (**1B**) was chosen. The reactions were optimized in terms of the catalyst amount, presence of a co-catalyst, type of solvent, temperature, and reagent stoichiometry based on the results of the reaction conditions for the synthesis of styryl-substituted DDSQ compounds in our previous article.¹⁵ The presented procedures ensure the efficiency of both reactions and also allow the undesirable polyarenes to be avoided without the need for any inhibitor addition. This was achieved due to the optimal stoichiometry of the reagents and the mild reaction conditions (refluxed DCM). After reaction condition optimization, a series of copolymers of stereoregular DDSQ-silylene-vinylene-arylene units was obtained. The polymeric products were thoroughly analyzed

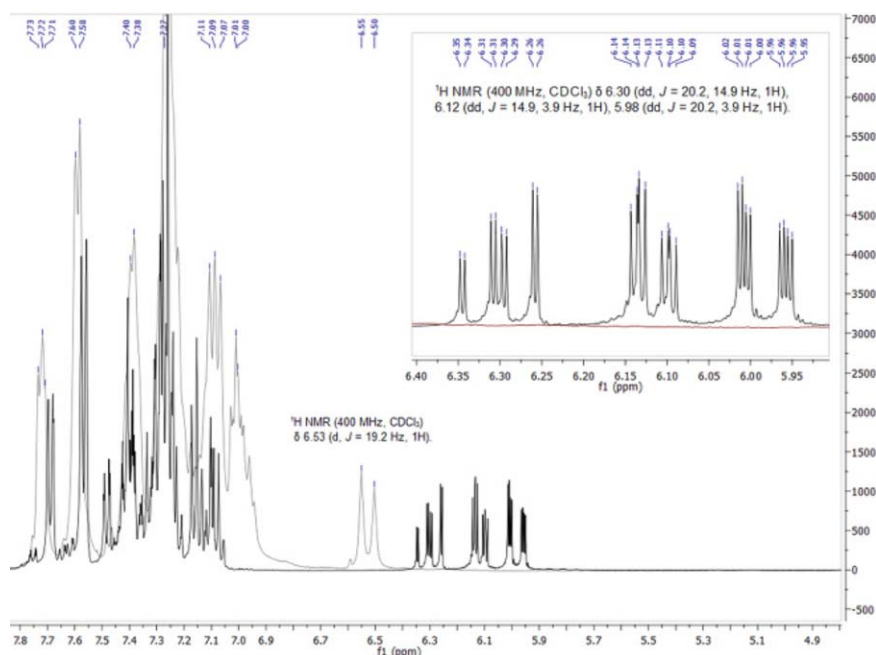


FIGURE 1 ^1H NMR-stacked spectra of **1B-1Ph-5** (gray) and **1B** (black). [Color figure can be viewed in the online issue, which is available at wileyonlinelibrary.com.]

via spectroscopic methods and their additional characteristics were also studied.

Polymer Characterization

Structure

The polymeric products were thoroughly characterized via ^1H , ^{13}C , ^{29}Si NMR using a comparison of their spectra with those of **DDSQ-2SiVi** substrates.

Figure 1 presents correlations between ^1H NMR spectra of **DDSQ-2SiVi** (**1B**) and its copolymeric (model) product with **DVB** (**1B-1Ph-5**) in the range of 4.9–7.9 ppm.

The chemical shifts of the vinylic protons of **1B** are between 6.35 and 5.95 ppm (the coupling constants of the protons are consistent with their geometrical placement). The ^1H NMR data of copolymeric product **1B-1Ph-5** confirm the appearance of new resonance lines (doublet) present at 6.53 ppm. This can be assigned to one of the vinylene protons in the vicinity of the DDSQ core (DDSQ-SiHC=) and the $J_{\text{HH}} = 19.2$ Hz corresponds to its *trans*-geometry with its twin vinylene proton next to the 1,4-substituted phenyl (**DVB**) ring. Another vinylene proton's doublet signal (in the vicinity of the **DVB** ring) is shifted to a higher range of the spectrum (in the range of the resonance lines of =CH bonds of phenyl and **DVB** group).

Figure 2 reveals a ^{13}C NMR spectra comparison of **DDSQ-2SiVi** (**1B**) and copolymer **1B-1Ph-5**. It can be noted that no resonance lines of free vinyl carbon moieties of **1B** (133.47 and 136.11 ppm) are present in the spectrum of **1B-1Ph-5** and new signals for the substituted vinylene C=C bonds appeared (137.68 and 147.52 ppm). However, the problem

with the (sp^2)C carbon of phenyl and arene group separation on the spectrum has arisen due to their chemical similarity. As a consequence, the (sp^2)C carbon signals in the experimental part are presented with no structural assignment.

With regards to the ^{29}Si NMR spectra, there is no substantial difference between the chemical surroundings of the silicon atoms in the vicinity of the vinyl group (Fig. 3) (in **1B** $\delta = -45.89$ ppm) and the DDSQ-vinylene-phenylene-vinylene

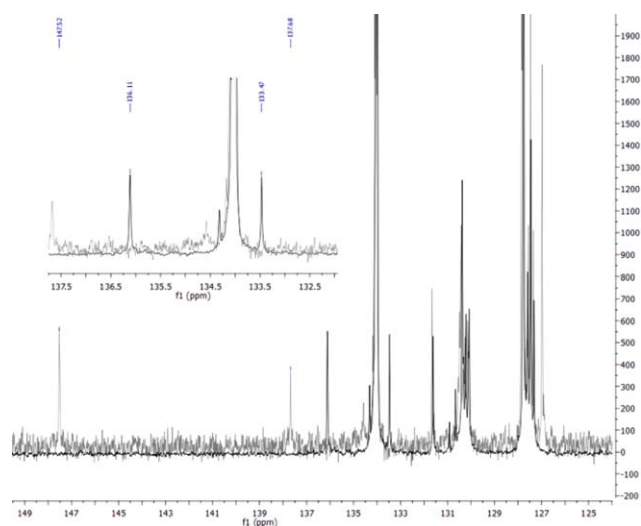


FIGURE 2 ^{13}C NMR-stacked spectra of **1B-1Ph-5** (gray) and **1B** (black). [Color figure can be viewed in the online issue, which is available at wileyonlinelibrary.com.]

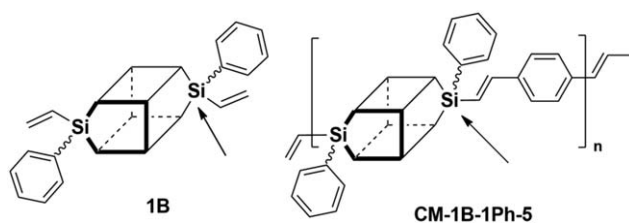


FIGURE 3 1B and 1B-1Ph-5 structural comparison in the aspect of chemical surrounding of marked silicon atoms.

group (in 1B-1Ph-5 $\delta = -44.62$ ppm). This is revealed in the small resonance line shift change.

Analogous proton, carbon and silicon NMR spectra were recorded for all copolymers presented in the publication (detailed data in the experimental section).

The FTIR spectrum of a model copolymer sample (1B-1Ph-5) also confirms the formation of the desired product and its structure (Fig. 4).

New bands formation at 1261, 808, and 781 cm^{-1} on the copolymer spectrum should be attributed to the bending vibrations of =C-H groups characteristic for *trans* disubstituted alkenes.

Gel Permeation Chromatography

Prepared polymers were analyzed by GPC to evaluate the effect of the co-monomers used, the type of catalytic process and its duration on their molecular weights and molecular weight distribution. The results obtained for polymers synthesized via SCC and ADMET copolymerization processes are summarized in Tables 1 and 2, respectively.

This influence is much more pronounced for ADMET than for SCC reactions. It can be observed that number average molecular weight (M_n) slightly increases with the use of heavier olefin and extension of the reaction time. This has not been observed in the case of SCC. It is also worth noticing that elongation of the reaction times of both processes

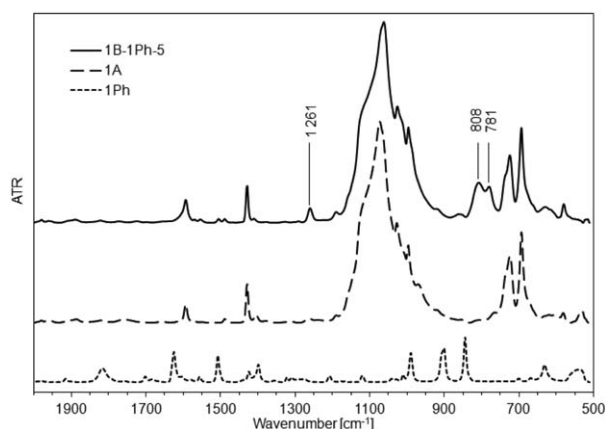


FIGURE 4 FTIR spectra of monomers (1B and 1Ph) and obtained copolymers (1B-1Ph-5).

TABLE 1 Molecular Weights of Polymers Obtained via SCC after 1- and 5-Day Synthesis

Polymer	M_n	M_w	PDI	Main Fraction (%)
1A-1Ph-1	10,800	16,100	1.5	72
1A-2Ph-1	11,000	16,300	1.5	81
1A-3Ph-1	10,500	15,500	1.5	77
1A-1Ph-5	10,957	20,333	1.9	74
1A-2Ph-5	10,393	17,784	1.7	61 ^a
1A-3Ph-5	10,200	18,200	1.8	87

^aPresent fraction of $M_n = 139,200$ and PDI = 2 (36%).

significantly influenced the weight average molecular weights (M_w) and subsequently the broadness of the molecular weight distribution of the obtained copolymers (increase of PDI). Although elongation of reaction times from 1 to 5 days does not always lead to an increase in the obtained polymer molecular weights, it enabled a reduction of low molecular fraction content in all cases (Fig. 5).

It is difficult to directly compare the obtained results with any other of the co-oligomeric systems studied, as to the best of our knowledge, this is the first example of this type of copolymer exploiting ADMET and SCC processes for their synthesis. However, Kakimoto et al. presented results on diynes hydrosilylation with dihydrofunctional DDSQ that led to synthesis of very similar linear polymers with a DDSQ spacer and π -conjugated aromatic fragments in between M_n weight (in a range of 11,900 to 29,100, and M_w/M_n values of 2.9–4.9) depending on diyne used.^{7(a)} On the basis of our results, it can be noted that metathetic ADMET copolymerization and SCC processes enable synthesis of copolymers of similar molecular weights, but with more precise control of molecular weight distributions.

Thermal Analysis (TGA and DSC)

Subsequently, all obtained copolymer samples were subjected to thermogravimetric studies. The analysis of the obtained thermograms made in N_2 atmosphere led to conclusion that most of the tested polymers are of relatively high thermal resistance with a char yield at 1000 $^\circ\text{C}$ of up to 70%. TG curves analyses of SCC and ADMET products (Figs. 6 and 7) led to the conclusion that there is a good correlation between the polymer thermal stability and its molecular weight or rather the content of the low molecular fraction.

TABLE 2 Molecular Weights of Polymers Obtained via ADMET Copolymerization after 1- and 5-Day Synthesis

Polymer	M_n	M_w	PDI	Main Fraction (%)
1B-1Ph-1	7,444	11,109	1.5	89
1B-2Ph-1	10,620	18,638	1.8	92
1B-1Ph-5	10,679	17,898	1.6	97
1B-2Ph-5	13,181	29,916	2.3	100

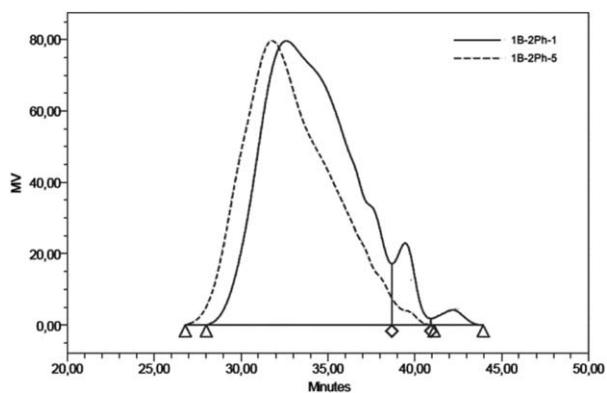


FIGURE 5 Model GPC chromatograms of **1B-2Ph** copolymers after 1 (solid) and 5 (dotted) days of **ADMET** copolymerization.

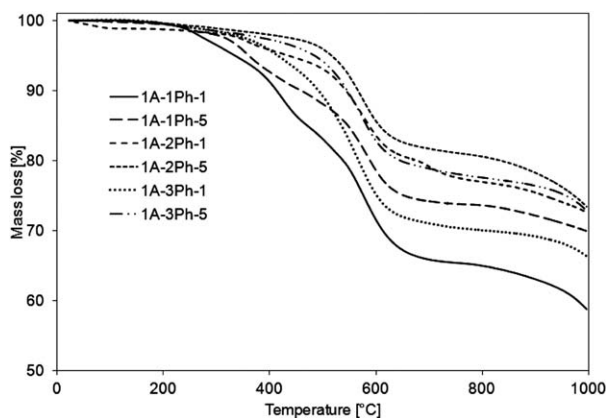


FIGURE 6 TGA curves (N_2) of obtained copolymers via **SCC**.

In all cases, significantly higher thermal stability was observed (Tables 3 and 4) for copolymers obtained after 5-day syntheses (**ADMET** or **SCC** processes).

The samples with the highest thermal stability were copolymers of 4,4'-divinylbiphenyl obtained by **ADMET** and **SCC**

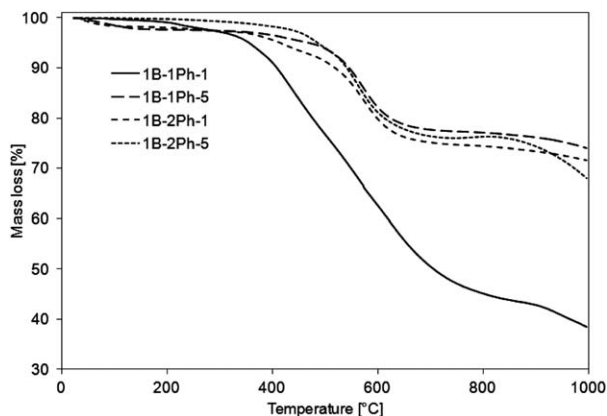


FIGURE 7 TGA curves (N_2) of obtained copolymers via **ADMET** copolymerization.

TABLE 3 Thermal Properties of copolymers obtained via **SCC** After 1 and 5-Day Synthesis Measured in N_2 and in the Air

Polymer	Temperature Loss ($^{\circ}C$)				Residue at 1000 $^{\circ}C$ (%)	
	5% (N_2)	5% (Air)	10% (N_2)	10% (Air)	(N_2)	(Air)
1A-1Ph-1	334	307	413	392	59	39
1A-2Ph-1	435	372	543	462	73	47
1A-3Ph-1	414	369	492	417	66	45
1A-1Ph-5	361	348	460	472	70	47
1A-2Ph-5	515	442	565	507	73	46
1A-3Ph-5	484	395	546	461	73	43

processes. High temperatures of 10% mass loss, reaching over 550 $^{\circ}C$ are characteristic for DDSQ copolymers irrespective of the comonomer or catalytic process used.^{7(e)} This effect can be attributed to the general fact of the high thermal stability of POSS compounds heaving phenyl groups.²¹

General tendency to the raise of the thermal stability of polymers synthesized in prolonged time (for both **ADMET** or **SCC** processes) can be also observed in the case of TG analysis conducted in the air atmosphere (Tables 3 and 4). The char yields observed at 1000 $^{\circ}C$ are, in this case, significantly lower and do not exceed 50%. It is also worth noticing that the final transition ends below 700 $^{\circ}C$ and this can be observed on Figures 8 and 9. Similar feature of lower 5 and 10% weight loss temperatures in the air was also observed in the case of polyimides with DDSQ in the main chain.^{7(g)}

The copolymer samples obtained after 5-day synthesis were also characterized with differential scattering calorimetry (Figs. 10 and 11). All the obtained curves were very analogous and no signals above 0 $^{\circ}C$ were observed. The only reversible signal observed for all samples located around -47 $^{\circ}C$ could probably be attributed to the glass transition with enthalpy relaxation.

TABLE 4 Thermal Properties of Copolymers Obtained via **ADMET** Copolymerization After 1 and 5-Day Synthesis Measured in N_2 and in the Air

Polymer	Temperature Loss ($^{\circ}C$)				Residue at 1000 $^{\circ}C$ (%)	
	5% (N_2)	5% (Air)	10% (N_2)	10% (Air)	(N_2)	(Air)
1B-1Ph-1	356	347	409	384	39	39
1B-2Ph-1	415	385	519	446	71	41
1B-1Ph-5	470	411	546	453	74	44
1B-2Ph-5	486	394	541	475	68	39

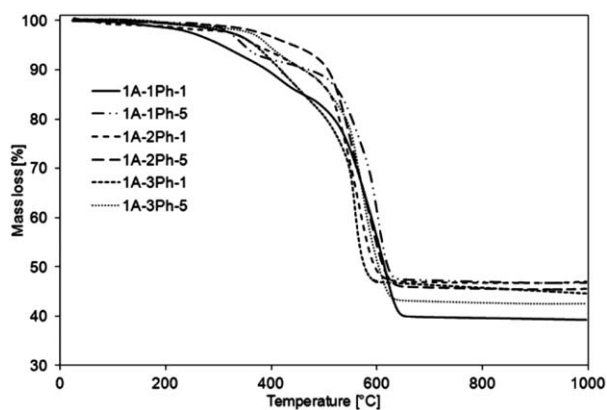


FIGURE 8 TGA curves (air) of obtained copolymers via SCC.

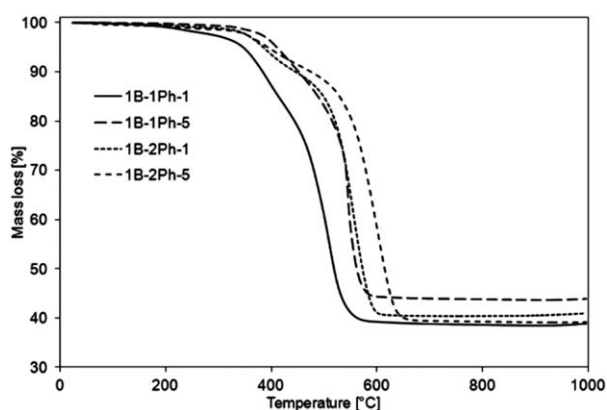


FIGURE 9 TGA curves (air) of obtained copolymers via ADMET copolymerization.

However, it could also indicate liquid crystalline properties of the obtained copolymers, as had been previously reported by Laine et al. for functionalized POSS compounds.²² This issue will be a subject of our further research.

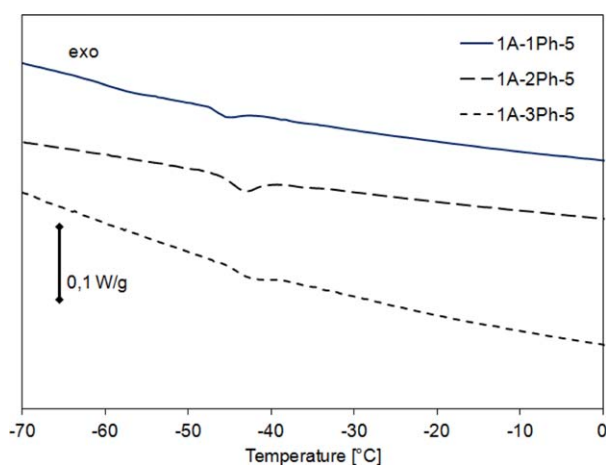


FIGURE 10 DSC curves of copolymers after 5-day synthesis via SCC.

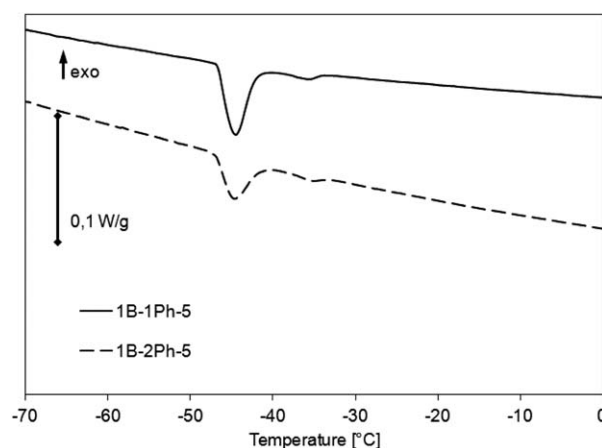


FIGURE 11 DSC curves of polymers after 5-day synthesis via ADMET copolymerization.

Surface Properties—Water Contact Angle

The obtained copolymers were also used for preparation of thin layer films on stainless steel plates with the spin-coating technique. Layers were prepared from THF solutions of various copolymer concentrations at a constant rotation speed of 100 rps in order to receive film of high quality. The measured film thickness was in the range of 120–150 μm . The most homogeneous coatings were obtained from the most diluted (5 wt %) copolymer solutions. Increasing the concentration of copolymer to 10 wt % resulted in the formation of rough coatings (Fig. 12).

For prepared steel plates covered with different copolymer films, their surface properties were characterized via WCA measurements (Table 5).

All of the obtained copolymer coatings were hydrophobic. The highest values of WCA were measured for **1A-3Ph-5** and **1B-2Ph-5** copolymers (104°) and the lowest for those of divinylbenzene (96°). WCA values increased with the use of “heavier” diolefin. Although the changes of WCA values are not very substantial, a distinct trend can be observed. As was to have been expected, the surface properties of the

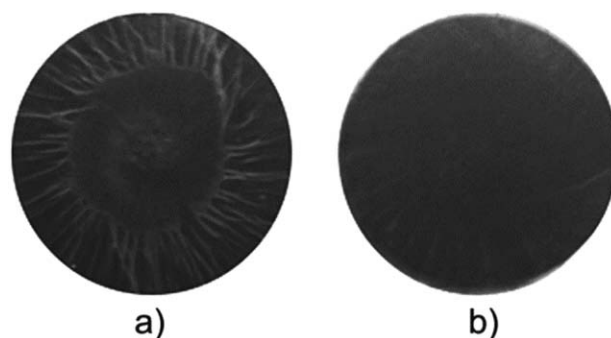


FIGURE 12 Stainless steel plates spin-coated with copolymer solutions in THF of different concentrations (a) for 10 wt % and (b) for 5 wt %.

TABLE 5 Water Contact Angle (WCA) Values for Stainless Steel Plates Coated with Various Copolymers

Sample	WCA (°)
Clean plate	81
1A-1Ph-5	96
1A-2Ph-5	102
1A-3Ph-5	104
1B-1Ph-5	97
1B-2Ph-5	104

obtained polymers were not influenced by the type of catalytic process.

SEM Imaging

Samples for SEM imaging were provided by dissolving a specimen of the desired compound in DCM and its precipitation in hexane. SEM images (Fig. 13) of **1A-1Ph-1** (a), **1A-2Ph-5** (b), **1A-3Ph-5** (c), **1B-1Ph-5** (d), and **1B-2Ph-1** (e) samples were taken. It can be noted that Figure 13(a–c) is substantially different from Figure 13(d–e). Specimens of compounds containing an Me group at 9 and 19 Si atom of **DDSQ-2SiVi** produced irregular grains with diameters ranging from about 1 to 10 microns. These irregular grains were built mostly from terrace oriented plates. The structure of these samples locally resembles a crystalline form.

Sample **1A-2Ph-5** built the terraces of the highest densities and smallest sizes. In samples **1A-1Ph-1** and **1A-3Ph-5** flat terraces with dimensions in the hundreds of nanometers could be observed. Between the grains large gaps can be noted.

Figure 13(d–e) presents the structures of samples containing Ph groups at 9 and 19 Si atom of **DDSQ-2SiVi** and are essentially different from those described above. These structures were composed of rounded particles with a diameter not exceeding one micron. No terraces were detected and the surface of the particles is smooth. In the case of **1B-2Ph-1** [Fig. 13(e)], it can be observed that most of the particles were almost spherical. This may originate from the higher symmetry of **1B** substrate (Ph groups at 9 and 19 Si atom of **DDSQ-2SiVi**) in comparison with **1A** which symmetry may be lower due to the presence of Me group at 9 and 19 Si atom. It is also abbreviated in the number of chemical shifts in the ^{29}Si NMR spectra of substrate **1B** and **1A**.^{15(b)}

The morphology of copolymers derived from **1A** suggested their potential local crystalline form. Selected sample **1A-3Ph-5** was subjected to wide-angle XRD measurement. Figure 14 shows the XRD profiles of **1A-3Ph-5** and substrate, that is, **DDSQ-2SiVi** (**1A**). In the diffraction curve of **1A** there were several sharp diffraction peaks that suggest its crystallinity. For the organic–inorganic copolymer **1A-3Ph-5**, the

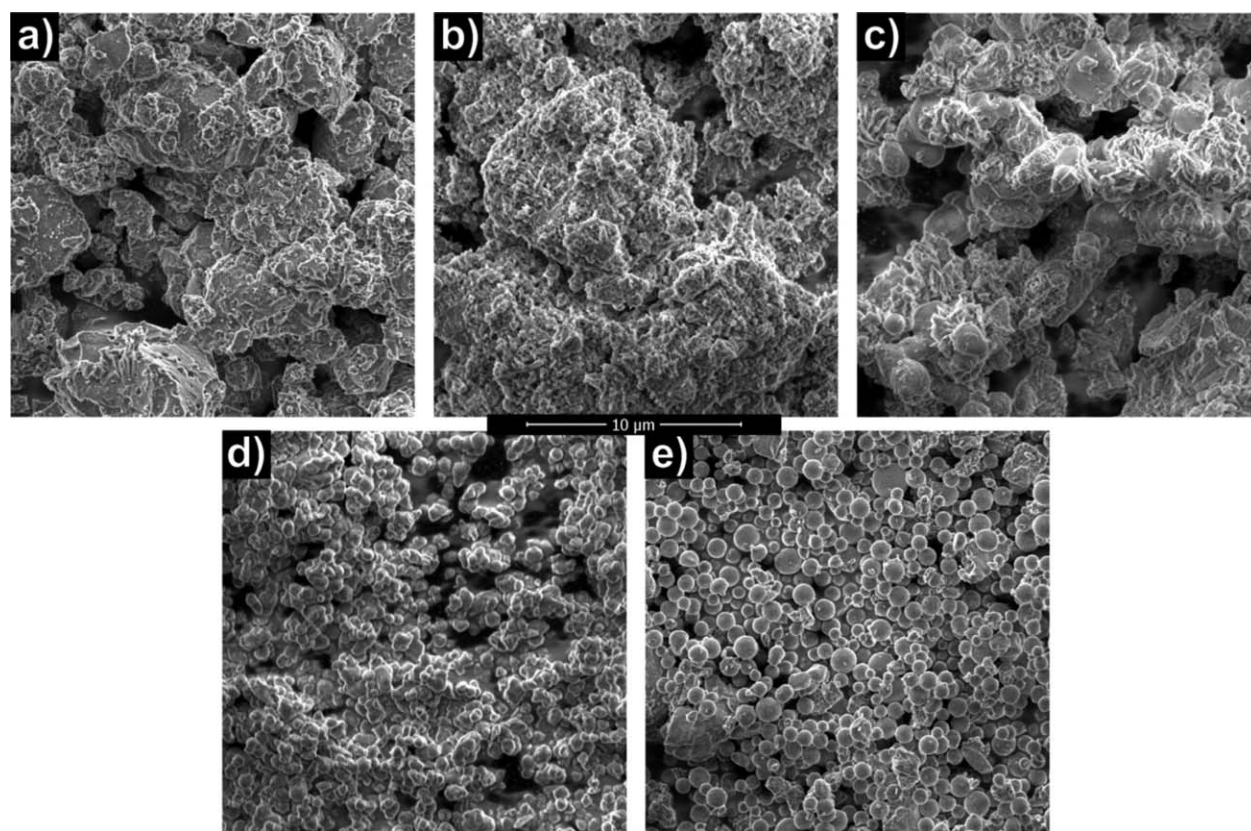


FIGURE 13 Scanning electron microscopy images of **1A-1Ph-1** (a), **1A-2Ph-5** (b), **1A-3Ph-5** (c), **1B-1Ph-5** (d), and **1B-2Ph-1** (e) samples. The scale in the middle applies to all images.

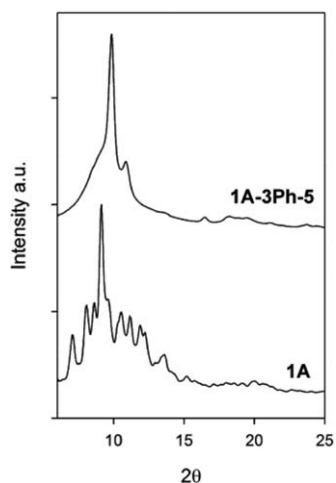


FIGURE 14 XRD profile of DDSQ-2SiVi (**1A**) and **1A-3Ph-5**.

XRD curves two rather sharp diffraction signals between $2\Theta = 10\text{--}12.5^\circ$ were detected that are slightly shifted to higher values of 2Θ in comparison with the substrate **1A**. The results of XRD may indicate that the organic–inorganic copolymers derived from **1A** tend to be crystallizable.^{7(k)}

Energy-dispersive X-ray spectroscopy (EDS) analysis was also performed for samples of **1A-2Ph-5** and **1B-1Ph-5**. The content and distribution of silicon, oxygen, and carbon atoms was analyzed in the selected specimens.

Distribution of these elements was detected to be uniform, which is a confirmation of the regularity of copolymers with the DDSQ fragment embedded in the main chain between the vinylene-arylene units. This could also prove the high level of homogeneity of the measured material.

Mechanical Analysis

Selected specimens were subjected to nanomechanical studies which involved the nanoindentation technique (described in the Measurements section). Figure 15 presents typical shapes of force–depth curves allowing determination of mechanical parameters. Slight differences in the shape of the curves between data points can be observed which can be

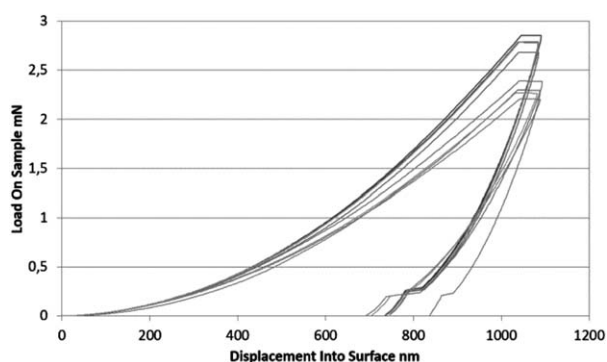


FIGURE 15 Force–depth curves for **1A-2Ph-5** sample. Each line presents a different measurement point on the sample surface.

TABLE 6 Young's Modulus of Analyzed Samples

Sample	Young Modulus (GPa)
1A-1Ph-1	1.81 ± 0.09
1A-2Ph-5	2.16 ± 0.22
1A-3Ph-5	2.02 ± 0.18
1B-1Ph-1	2.27 ± 0.18
1B-1Ph-5	2.44 ± 0.21
1B-2Ph-1	2.67 ± 0.30
1B-2Ph-5	2.72 ± 0.20

attributed to difficulties in obtaining a sample surface with a very low roughness.

Young's modulus data for the designated samples also measured with the nanoindentation technique are presented in Table 6. A statistical dispersion of results is assumed as a standard deviation.

The measured values of Young's modulus varied between 1.8 and 2.7 GPa and are a little more than those describing polyolefins which could be explained by the presence of a rigid silsesquioxyl block. It may be noted that copolymers containing **1B** fragment in the chain, that is, Ph group at 9 and 19 Si atom of DDSQ-2SiVi, exhibit a higher Young's modulus factor than those with the **1A** unit.

This may be associated with the presence of more sterically demanding, flat phenyl moieties in comparison with the methyl group. A considerable effect of reaction time elongation on the above discussed modulus can also be observed, which could be clearly assigned to the longer chains of the resulting copolymers.

CONCLUSIONS

The above results demonstrate the complementarity and fidelity of the **SCC** and **ADMET** reactions as a tool for the stereoselective synthesis of a new class of vinylene–arylene copolymers containing DDSQ in the main chain. The ¹H NMR analysis confirms quantitative formation of trans-geometry of the resulting vinylene bond between DDSQ and arene units. GPC measurements confirm that elongation of reaction times has improved the average molecular weights (M_w) of copolymers. TG analyses have proved the high level of thermal resistance of the obtained systems, reaching over 550 °C, which is in close correlation with DDSQ copolymers. The WCA values do not depend on the method of copolymer synthesis, but on the structure of the arene fragment and an increase in this tendency can be observed with the increase in diolefin weight. These mechanical studies reveal that these new copolymeric materials possess slightly higher Young's modulus values than is the case with polyolefins. The effect of DDSQ-2SiVi type, that is, the presence of a Ph group at the functional Si atom in the DDSQ unit, and time elongation was also discussed.

ACKNOWLEDGMENT

The authors gratefully acknowledge financial support from the National Science Center (Poland) (SONATA Project No. DEC-2012/05/D/ST5/03348, MAESTRO Project No. DEC-2011/02/A/ST5/00472).

REFERENCES AND NOTES

- (a) D. B. Cordes, P. D. Lickiss, F. Rataboul, *Chem. Rev.* **2010**, *110*, 2081–2173; (b) C.-M. Leu, Y.-T. Chang, K.-H. Wei, *Macromolecules* **2003**, *36*, 9122–9127; (c) C.-M. Leu, Y.-T. Chang, K.-H. Wei, *Chem. Mater.* **2003**, *15*, 3721–3727.
- (a) Y. Morimoto, K. Watanabe, N. Ootake, J. Inagaki, K. Yoshida, K. Ohguma, EP 1 428 795 (A1), US 7 169 873 (B2), US 7 449 539 (B2); (b) K. Yoshida, *Polym. Preprints Japan*, **2003**, *52*, 316; (c) N. Ootake, K. Yoshida, US 2006/0155091(A1).
- (a) A. C. Kucuk, J. Matsui, T. Miyashita, *Langmuir* **2011**, *27*, 6381–6388; (b) A. C. Kucuk, J. Matsui, T. J. Miyashita, *Colloid Interface Sci.* **2011**, *355*, 106–114; (c) A. C. Kucuk, J. Matsui, T. Miyashita, *J. Mater. Chem.* **2012**, *22*, 3853–3858; (d) A. C. Kucuk, J. Matsui, T. Miyashita, *Thin Solid Films* **2013**, *534*, 577–583.
- B. Seurer, V. Vij, T. Haddad, J. M. Mabry, A. Lee, *Macromolecules* **2010**, *43*, 9337–9347.
- M. Kohri, J. Matsui, A. Watanabe, T. Miyashita, *Chem. Lett.* **2010**, *39*, 1162–1163.
- J. Espinas, J. D. A. Pelletier, E. Abou-Hamad, L. Emsley, J.-M. A. Basset, *Organometallics* **2012**, *31*, 7610–7617.
- (a) M. Seino, T. Hayakawa, Y. Ishida, M. Kakimoto, K. Watanabe, H. Oikawa, *Macromolecules* **2006**, *39*, 3473–3475; (b) K. Yoshida, T. Hattori, N. Ootake, R. Tanaka, H. Matsumoto, in “Silsesquioxane-based polymers: synthesis of phenylsilsesquioxanes with double-decker structure and their polymers” Silicon Based Polymers. Advances in Synthesis and Supramolecular Organization; F. Ganachaud, S. Boileau, B. Boury, Ed.; Springer: London-New York, **2008**, pp. 205–211; (c) A. Watanabe, S. Tadenuma, T. Miyashita, *J. Photopolym. Sci. Technol.* **2008**, *21*, 317–318; (d) M. Aminuzzaman, A. Watanabe, T. Miyashita, *J. Mater. Chem.* **2008**, *18*, 5092–5097; (e) M. Miyasaka, Y. Fujiwara, H. Kudo, T. Nishikubo, *Polym. J.* **2010**, *42*, 799–803; (f) S. Wu, T. Hayakawa, R. Kikuchi, S. J. Grunzinger, M. Kakimoto, H. Oikawa, *Macromolecules* **2007**, *40*, 5698–5705; (g) S. Wu, T. Hayakawa, M. Kakimoto, H. Oikawa, *Macromolecules* **2008**, *41*, 3481–3487; (h) W. Zhang, J. Xu, X. Li, G. Song, J. Mu, *J. Polym. Sci. Part A: Polym. Chem.* **2014**, *52*, 780–788; (i) L. Wang, Ch. Zhang, S. Zheng, *J. Mater. Chem.* **2011**, *21*, 19344–19352; (j) K. Wei, L. Wang, S. Zheng, *Polym. Chem.* **2013**, *4*, 1491–1501; (k) K. Wei, L. Wang, S. Zheng, *J. Polym. Sci. Part A: Polym. Chem.* **2013**, *51*, 4221–4232.
- For review see: (a) C. Pietraszuk, P. Pawluć, B. Marciniak, In *Handbook on Metathesis*; R. Grubbs and D. J. O’Leary, Ed.; **2015**, Vol. 2, Chapt. 9, 583–631; (b) B. Marciniak, *Acc. Chem. Res.* **2007**, *40*, 943–952; (c) B. Marciniak, *Coord. Chem. Rev.* **2005**, *249*, 2374–2390; (d) B. Marciniak, C. Pietraszuk, In *Green Metathesis Chemistry. Great Challenges in Synthesis Catalysis and Nanotechnology*; V. Dragutan, A. Demonceau, I. Dragutan, E. S. Finkelshtein, Eds.; Springer, Berlin, **2010**; p. 157.
- (a) Y. Itami, B. Marciniak, M. Kubicki *Chem. A. Eur. J.* **2004**, *10*, 1239; (b) J. Waehner, B. Marciniak, P. Pawluć *Eur. J. Inorg. Chem.* **2007**, 2975; (c) P. Žak, C. Pietraszuk, B. Marciniak, G. Spolnik, W. Danikiewicz *Adv. Synth. Catal.* **2009**, *351*, 2675; (d) P. Žak, B. Marciniak, M. Majchrzak, C. Pietraszuk *J. Organometal. Chem.* **2011**, *696*, 887.
- S. Sulaiman, A. Bhaskar, J. Zhang, R. Guda, T. Goodson, III, R. M. Laine, *Chem. Mater.* **2008**, *20*, 5563.
- H. Araki, K. Naka, *J. Polym. Sci. Part A: Polym. Chem.* **2012**, *50*, 4170–4181.
- (a) G. Cheng, N. R. Vautravers, R. E. Morris, D. J. Cole-Hamilton, *Org. Biomol. Chem.* **2008**, *6*, 4662; (b) N. R. Vautravers, P. Andre, A. M. Z. Slavin, D. J. Cole-Hamilton, *Org. Biomol. Chem.* **2009**, *7*, 717; (c) N. R. Vautravers, P. Andre, D. J. Cole-Hamilton, *J. Mater. Chem.* **2009**, *19*, 4545.
- F. J. Feher, D. Soulivong, A. G. Eklund, K. D. Wydham, *Chem. Commun.* **1997**, 1185.
- M. Lo Conte, S. Staderini, A. Chambery, N. Berthet, P. Dumy, O. Renaudet, A. Marra, A. Dondoni, *Org. Biomol. Chem.* **2012**, *10*, 3269–3277.
- (a) P. Žak, B. Dudziec, B. Marciniak, US Pat. Appl. US 14 640 618 (**2015**), EP 15461513.2; (b) P. Žak, B. Dudziec, M. Kubicki, B. Marciniak, *Chem. Eur. J.* **2014**, *20*, 9387–9393.
- C. S. Yi, D. W. Lee, Y. Chen, *Organometallics* **1999**, *18*, 2043–2045.
- N. Ootake, K. Yoshida, K. Watanabe, Y. Yamaryo US 8 173 758 (B2).
- Agilent Technologies, Program CrysAlisPro, ver.171.37.35, Yarnton, Oxfordshire, England, **2014**.
- M. Majchrzak, S. Kostera, M. Kubicki, I. Kownacki, *Dalton Trans.* **2013**, *42*, 15535–15539.
- C. Pietraszuk, H. Fischer, *Chem. Commun.* **2000**, 2463–2464.
- D. B. Cordes, P. D. Lickiss in *Applications of Polyhedral Oligomeric Silsesquioxanes, Advances in Silicon Science 3*, C. Hartmann-Thompson Ed., Springer, **2011**, 47–134.
- A. Sellinger, R. M. Laine, V. Chu, C. Vlney, *J. Polym. Sci. Part A: Polym. Chem.* **1994**, *32*, 3069–3089.